MINERAL MAPPING IN THE MARYSVALE VOLCANIC FIELD, UTAH USING AVIRIS DATA

Barnaby W. Rockwell, Roger N. Clark, Charles G. Cunningham,
Stephen J. Sutley, Carol A. Gent,
Robert R. McDougal, K. Eric Livo, and Raymond F. Kokaly

United States Geological Survey
Denver, Colorado
http://speclab.cr.usgs.gov

1. Introduction

This paper presents the results of AVIRIS-based mineral mapping in the Marysvale volcanic field, Sevier and Piute Counties, Utah. This work was performed as a part of the USGS-EPA Utah Abandoned Mine Lands (AML) Imaging Spectroscopy Project, in which spectroscopic imaging and analysis are being employed for watershed evaluation in areas of past and present mining activity. The project will map surface mineralogy to identify natural and man-made sources of acid generation as well as carbonate and chlorite-bearing lithologies which may provide acid buffering effects. Longer-term goals of the project include the application of the AVIRIS mineral maps to ore deposit studies and the generation of geo-environmental models for different ore deposit types.

2. Geologic Setting, Hydrothermal Alteration, and Ore Deposits

The Marysvale volcanic field (Figure 1) is located in southwestern Utah in the High Plateaus transition zone between the Colorado Plateau and Basin and Range provinces. The field lies at the eastern end of the Pioche-Marysvale igneous belt which is comprised of Cenozoic igneous rocks and is underlain by a large batholith complex. This paper will focus on mineral mapping results obtained from the Antelope Range (Figure 2), a group of low hills located five kilometers northeast of the town of Marysvale. These hills are the site of major deposits of volcanogenic uranium and replacement alunite. The hills are separated from the Tushar Mountains to the west by Marysvale Canyon, where the Sevier River has cut downwards through volcanic rocks along a series of entrenched meanders.

The volcanic rocks of the Marysvale region unconformably overlie a thick sequence of Paleozoic, Mesozoic, and lower Tertiary sedimentary rocks. The Cenozoic geologic history and ore deposits of the Marysvale volcanic field are summarized in Figure 3. In the Antelope Range, intermediate composition volcanic rocks of Tertiary age were intruded by quartz monzonite stocks around 23 m.y. ago (Cunningham et al., 1984). The stocks are localized between en echelon systems of NNW-trending faults where east-west extension was accommodated along a set of northwards-trending faults. The intrusion of these stocks (labeled “Central Intrusive” on Figure 4) initiated convective fluid flow in a series of rising hydrothermal plumes spaced at roughly even intervals around the periphery of the stocks. The locations of the plumes appear to be structurally controlled by faults (Kerr et al., 1957). These plumes created discrete zones, or “cells,” of intense acid sulfate alteration which were mapped with remote sensing techniques by the airborne NASA Bendix multispectral scanner (Podwysocki et al., 1983).

Cunningham (et al., 1984) proposed a genetic model for the deposits of replacement alunite which occur in the cores of several of the hydrothermal alteration cells in the Antelope Range. The model suggests that the alteration cells were formed in shallow, steam-dominated hydrothermal environments in which the near-surface oxidation of hypogene H_2S is the principal factor controlling mineralization. The cells exhibit strong horizontal and vertical zonation. Horizontal zonation in the cells is concentric in pattern and grades outwards from an alunitic core to an alunite-kaolinite transition zone, to a kaolinite zone, and finally to an envelope of propylitic alteration which merges into regionally propylitized rocks. Vertical zonation within the alteration cells consists of an upwards transition from a reduced, pyrite-rich, propylitically-altered feeder zone formed below the paleoground-water table, to the alunite zone formed in the presence of atmospheric oxygen near the paleoground-water table, through zones of hypogene jarosite and hematite, and finally to a cap of hydro-fractured silica formed at or near the paleoground surface. Sulfur isotopic data support a hypogene origin for the steam-heated jarosite at Marysvale (Rye and Alpers, 1997).

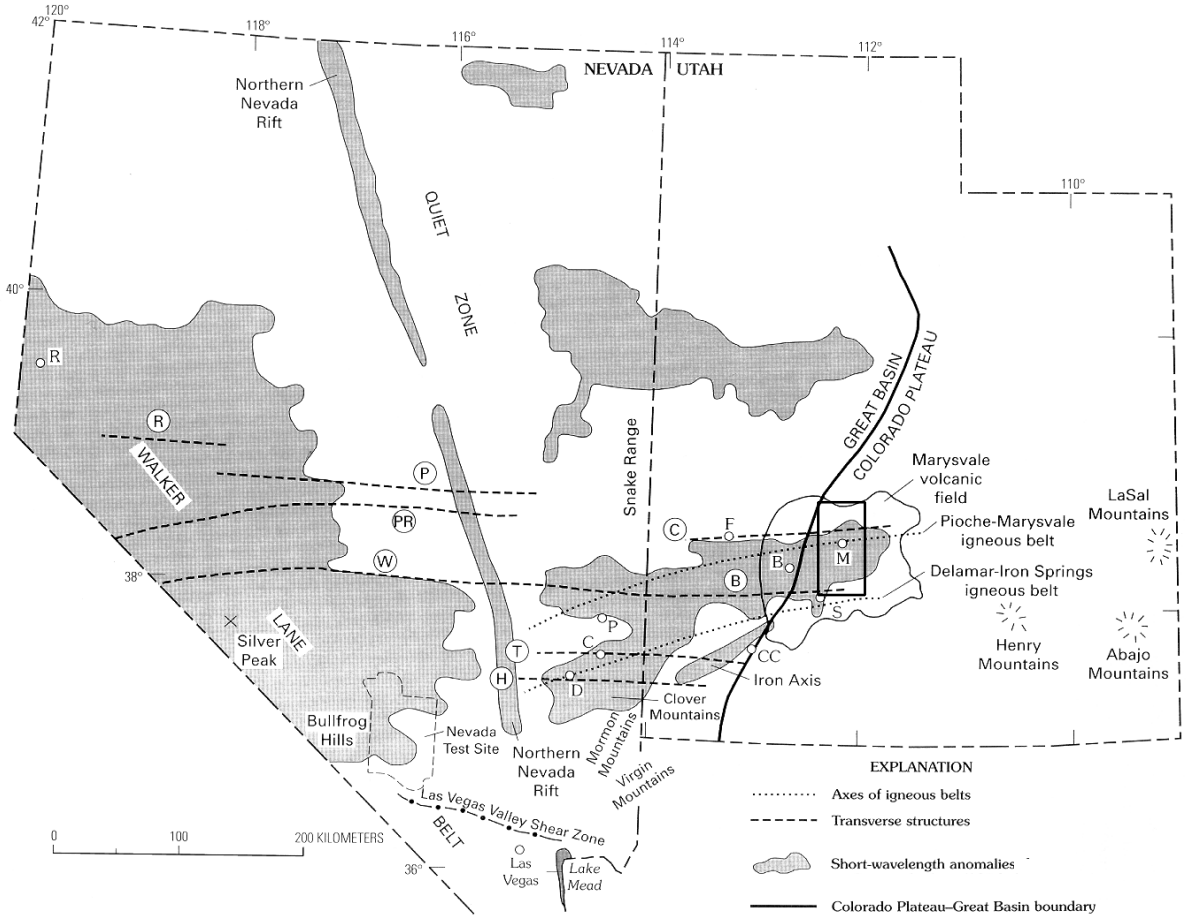

Figure 1. Major igneous and tectonic features of Nevada and Utah. Towns and cities: R, Reno; C, Caliente; P, Pioche; D, Delamar; F, Frisco; M, Marysvale; B, Beaver; S, Spry; CC, Cedar City. Transverse structures (circled): R, Rawhide; P, Prichards Station; PR, Pancake Range; B, Blue Ribbon; W, Warm Springs; C, Cove Fort; T, Timpahute; H, Helene. Rectangle indicates area of AVIRIS data coverage shown in Figure 2. Modified from Rowley et al. (1998).

The replacement alunite deposits of the Antelope Range were mined for potassium sulfate fertilizer during World War I and as a source of aluminum during World War II. Small lode gold deposits were also mined in this area. Most mining in the Antelope Range took place after World War II and exploited hydrothermal U-Mo-F vein deposits associated with 18 million year old stocks located immediately to the south of the Central Intrusive (Figure 4) (Cunningham et al., 1998). Rich deposits of hematite in the upper parts of the Yellow Jacket cell (sometimes referred to as "Iron Hat") were mined for iron ore.

3. Environmental Impacts of Mining Activity

One of the principal objectives of the Utah AML project is to remotely identify occurrences of iron sulfate minerals such as jarosite, schwertmannite, and copiapite in mine waste rock piles and tailings from smelters and other ore processing facilities. Jarosite can form by the subaerial supergene oxidation of the common gangue mineral pyrite, a process which involves the production of H_2SO_4. This acid can in turn mobilize heavy metals present in the local environment and transport them into ground- and surface-water systems, creating a potential health hazard. The presence of iron sulfate minerals is thus an indicator of acid production in the environment

Little environmental impact due to mining is present in the Antelope Range outside of the small "Central Mining Area" (labeled "X" on Figure 4) from which uranium was extracted, and no sizeable ore processing/smelting operations were located there. The abundance of heavy metals in the alunite deposits of the Antelope Range can be

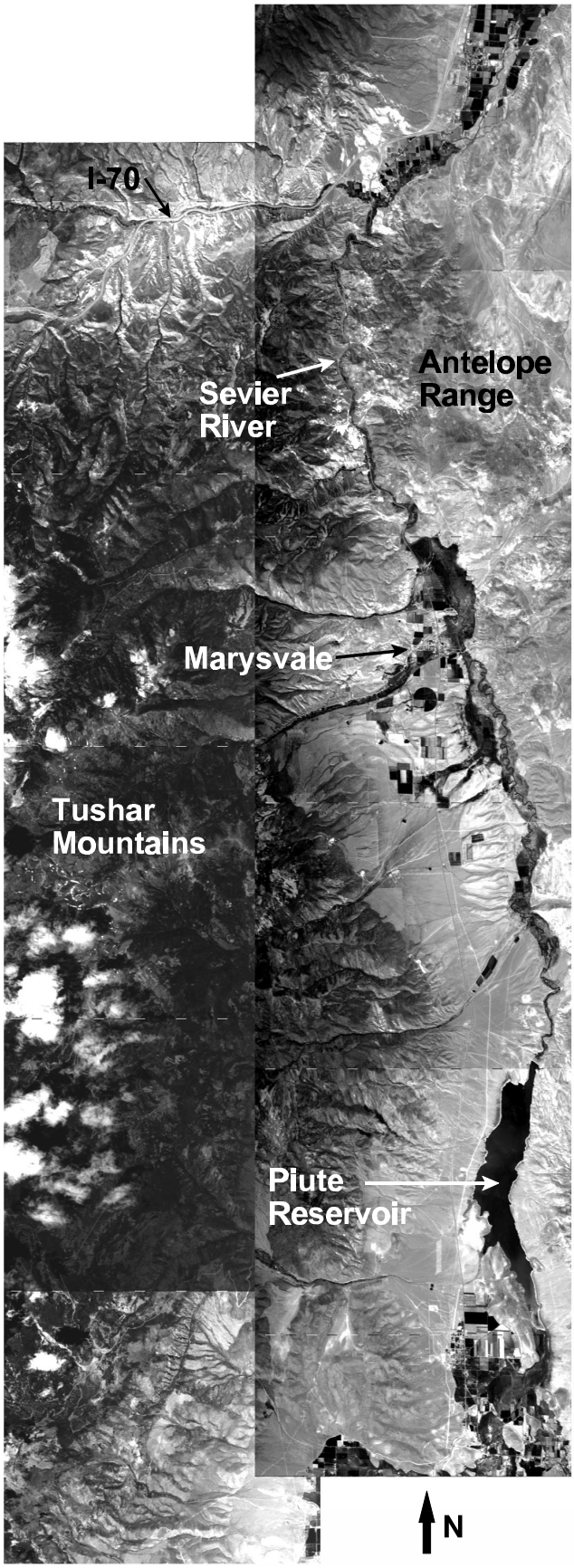

Figure 2. Mosaic of AVIRIS scenes covering the Tushar Mountains, Antelope Range, and Sevier River valley.

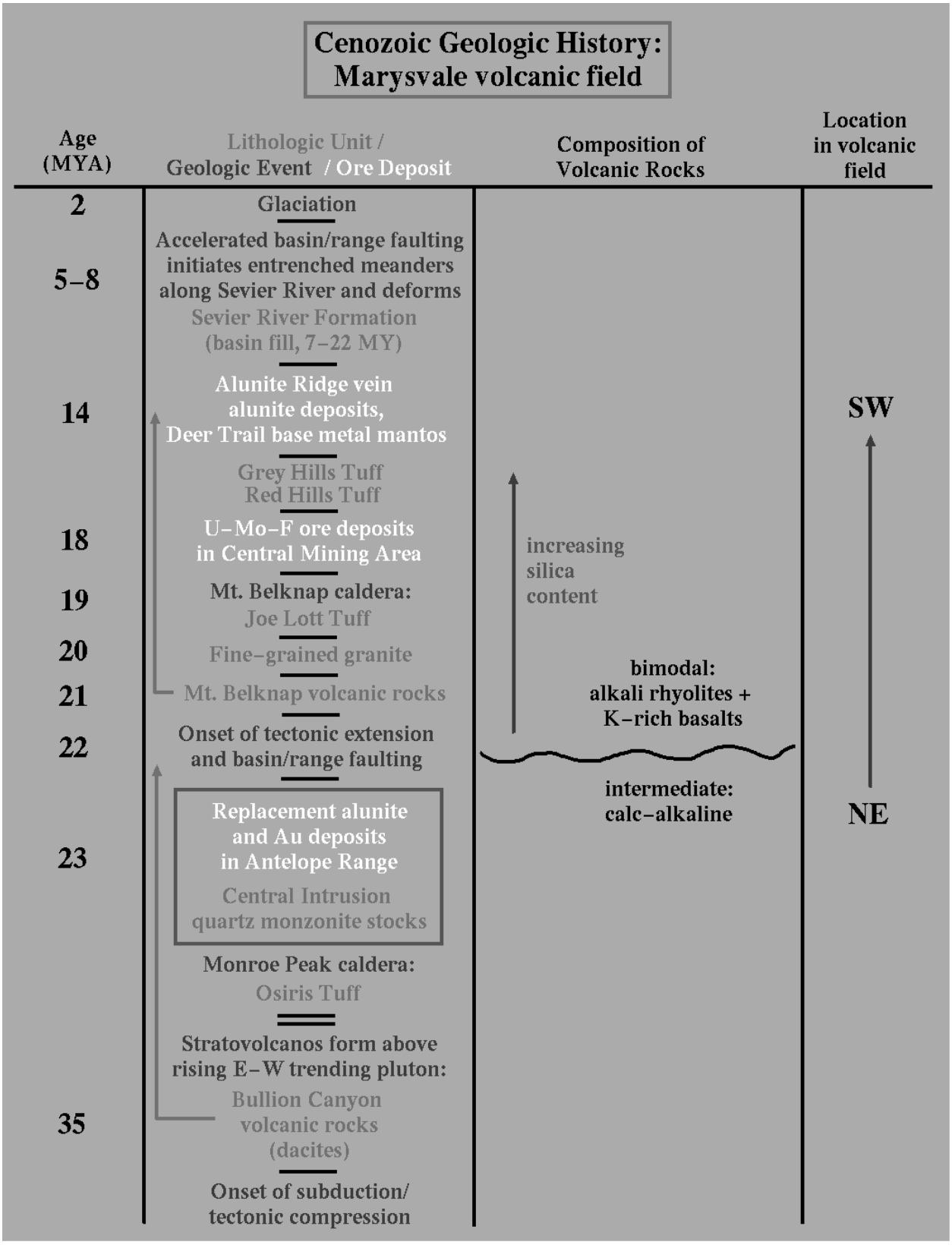

Figure 3. Cenozoic geologic history, Marysvale volcanic field, Utah.

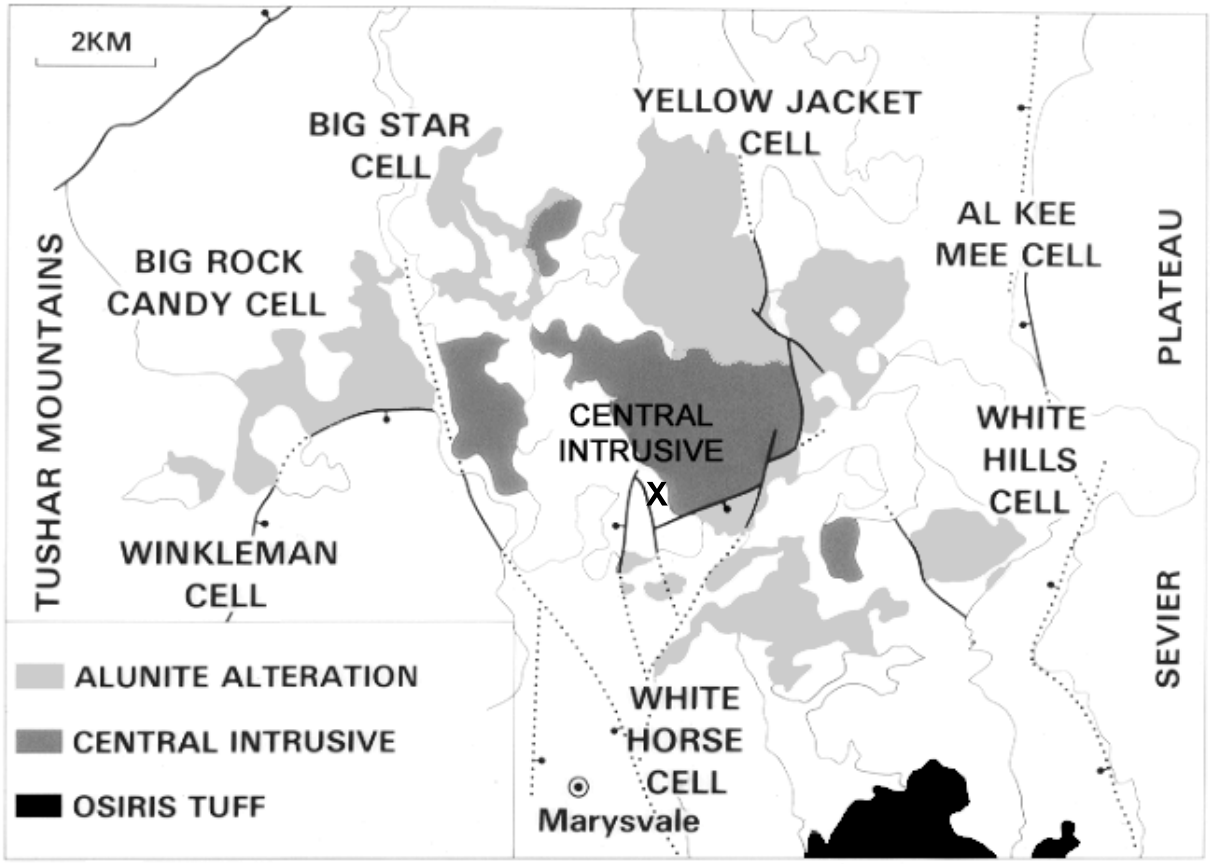

Figure 4. Map of principal geologic units and replacement alunite alteration in the Antelope Range, Marysvale volcanic field, Utah. Alunite-bearing hydrothermal alteration cells are distributed around a 23 m.y. old stock of quartz monzonite, labeled the "Central Intrusive." The Sevier River flows northwards through Marysvale Canyon between the Big Rock Candy Mountain and Big Star cells. X, Central uranium Mining Area.

considered to be low. Most mines in the Marysvale region exploited gold and base metal deposits in the east-central part of the Tushar Mountains (see **http://speclab.cr.usgs.gov/earth.studies/Utah-1/utav200c.jpg**) southwest of the town of Marysvale, and it is at these mine sites where the potential for the presence of heavy metals available for transport into the environment is highest.

4. AVIRIS Data Reflectance Calibration

High altitude AVIRIS imagery was acquired over the Marysvale region on August 5, 1998 (Figure 2). The AVIRIS data were calibrated to reflectance using a two step process (Clark et al., 1999). In the first step, the data are corrected using an algorithm (ATREM, Gao and Goetz, 1990 and Gao et al., 1992) that estimates the amount of atmospheric water vapor in the spectrum of each pixel independently, as compared with an atmospheric model. The algorithm uses this information to reduce the effects of absorptions caused by atmospheric water vapor on a pixel-by-pixel basis. This step also includes characterizing and removing the effects of Rayleigh and aerosol scattering in the atmosphere (path radiance), and a correction for the solar spectral response relative to wavelength. The second step requires the in situ spectral characterization of a ground calibration site which is present in the AVIRIS data coverage. The field site used for the calibration of the Marysvale AVIRIS data was the boat ramp at the northern end of the Piute Reservoir (Figure 2, see also **http://speclab.cr.usgs.gov/earth.studies/Utah-1/tushar.LABELS.tgif.jpg**). Additional areas of known composition were used to verify and further refine the accuracy of the calibration and to derive any residual path radiance correction.

5. Spectral Analysis

The USGS Tetracorder expert system was used for spectral analysis of the AVIRIS data (Clark et al., 1990, 1991, 1995). This semi-automated system compares the spectrum of each pixel in the AVIRIS data to a digital library of standard laboratory spectra of minerals, mineral mixtures, man-made materials, and vegetation. Each pixel is mapped separately for several different groups of surface materials, so that several maps can be generated for each AVIRIS dataset, including a map of iron-bearing minerals (0.35 to 1.35 micron spectral region), a map of phyllosilicate, sulfate, carbonate, and sorosilicate minerals (1.45 to 2.5 micron spectral region), and maps of man-made materials, snow, water, and vegetation. Mapping results are verified by both field checking and interactive comparison of AVIRIS spectra with library spectra. Selected mapping results were verified using XRD analysis.

6. Results and Discussion

The results of this paper are focused on the AVIRIS mineral mapping results from the Big Rock Candy Mountain, Big Star, and Yellow Jacket cells (see Figure 4). The White Hills cell and the eastern half of the Al Kee Mee cell were not covered by the 1998 AVIRIS data.

Plate 1 shows the map of iron-bearing minerals and mineral mixtures which were mapped from the Marysvale AVIRIS data. Extensive exposures of non-anthropogenic jarosite were mapped next to the Sevier River at Big Rock Candy Mountain (A, Plate 1), and along the southwestern flank of the Yellow Jacket cell (B, Plate 1) at higher elevations in the heart of the Antelope Range. Samples from both locations were confirmed to contain jarosite by XRD analysis. Figure 5 shows average AVIRIS spectra of the jarosites from these two locations, which were differentiated via the AVIRIS mapping. The small black arrows indicate the ferric iron absorption bands used for the automated, quantitative comparison of AVIRIS spectra with laboratory reference spectra. The spectrum from Big Rock Candy Mountain represents a fine-grained coating of jarosite produced through the subaerial supergene oxidation of disseminated pyrite present within the propylitically altered feeder zone of the cell. The other spectrum in Figure 5 was sampled from argillically altered rocks of the Yellow Jacket cell (B, Plate 1). Abundant lichen and sagebrush cover the flanks of the Yellow Jacket cell, as is evident by the noticeable deepening of the chlorophyl absorption band at 0.67 microns present in these AVIRIS spectra. XRD analysis has determined that these rocks contain abundant alunite and kaolinite, but no pyrite, suggesting that the jarosite exposed at the Yellow Jacket cell is hypogene in origin. The variation in spectral shape between the two types of jarosite could be due to coarser grain size and/or increased amounts of goethite in the sample from the Yellow Jacket cell.

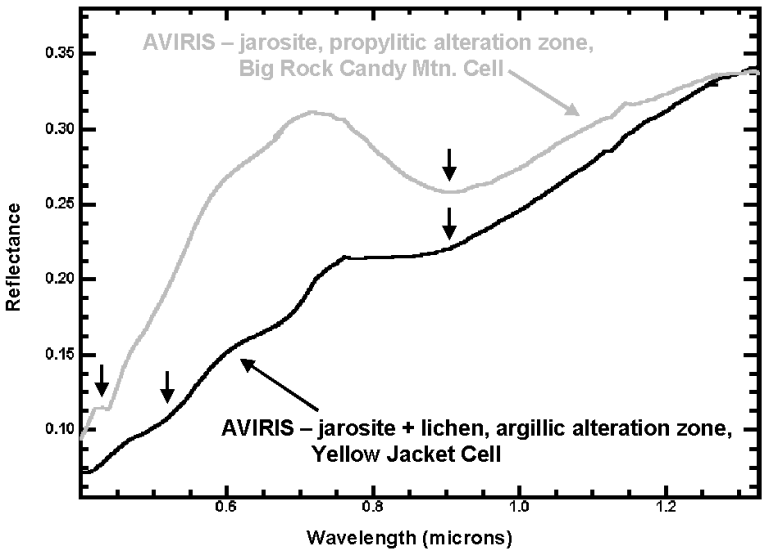

Figure 5. Average AVIRIS spectra of jarosites from the Antelope Range. See text for explanation.

Exposures of medium to coarse-grained hematite were mapped on the upper parts of the Yellow Jacket cell (C, Plate 1), and are interpreted as primary hypogene hematites associated with the original alteration. Chlorites associated with pyrite-poor distal propylitic alteration of the Central Intrusive wall rocks are present around the edges of the Big Rock Candy Mountain cell where exposed in Marysvale Canyon by the downcutting of the Sevier River (D, Plate 1).

Plate 2 shows the mineral mapping results from the 1.4 - 2.5 micron spectral range. The alunites, kaolinites, and dickites of the advanced argillic alteration zones in the Yellow Jacket cell are evident (A, Plate 2).

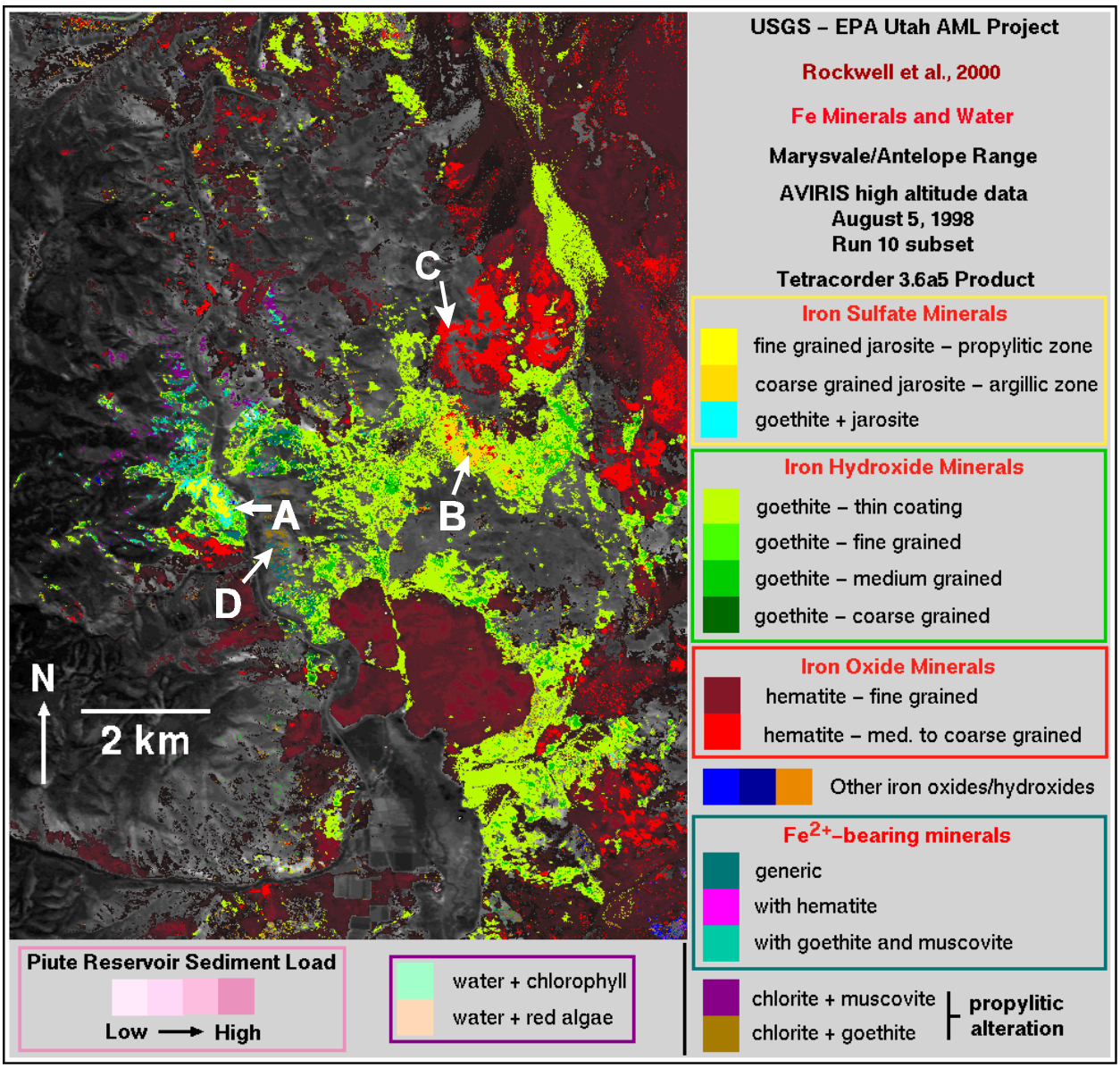

Plate 1. Map of Fe-bearing minerals (0.35 to 1.35 micron spectral region) in the Antelope Range derived from Tetracorder analysis of the AVIRIS data. Sediment load in the Piute Reservoir (not shown here) was stratified by matching spectra of measured amounts of clay mixed with water to the AVIRIS data. See text for description of labelled areas.

These minerals are partially masked in the central and western parts of the cell by an overlying cap of chalcedony and hematite.

The Sevier River has eroded downwards through the advanced argillic zone of the Big Rock Candy Mountain cell, stripping away most of the alunite and exposing the pyrite-rich propylitically altered feeder zone of the cell. Intimate mixtures of jarosite, illite, gypsum and clay minerals (dickite and kaolinite) were mapped on the flanks of Big Rock Candy Mountain (B, Plate 2). Where calcite was abundant in the propylitically altered rocks in the feeder zone of the cell, supergene oxidation has produced gypsum in addition to jarosite. Residual alunite and clay minerals were mapped on the top of Big Rock Candy Mountain above the propylitic zone.

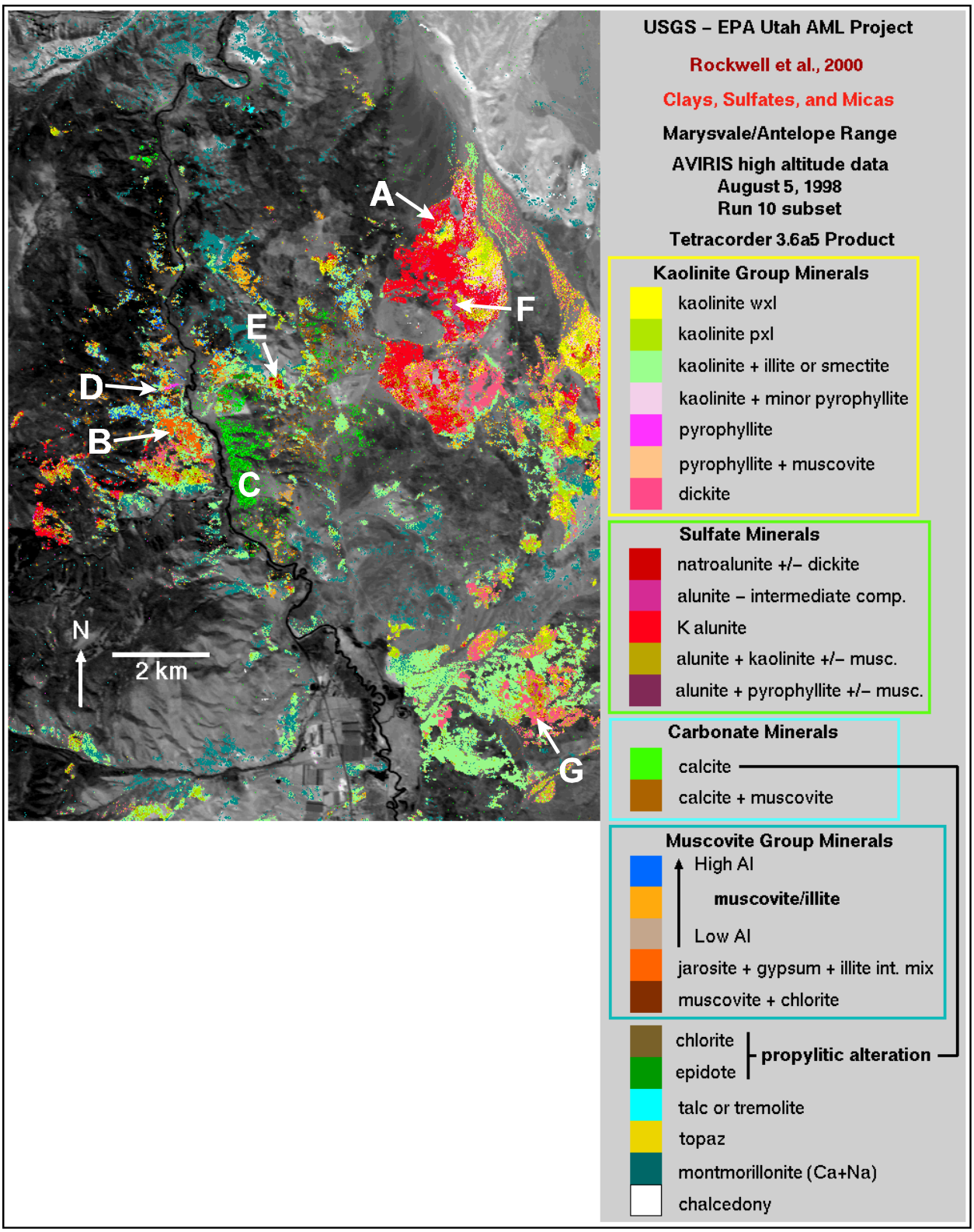

Plate 2. Map of phyllosilicate, sulfate, carbonate, and sorosilicate minerals (1.45 to 2.5 micron spectral region) derived from the AVIRIS data. See text for description of labeled areas.

Extensive exposures of dickite, a high temperature polymorph of kaolinite, were mapped in the southern half of the Yellow Jacket cell, and in the central parts of the Big Rock Candy Mountain and White Horse cells. Dickite appears to form in high temperature, steam-dominated hydrothermal environments in which systems of pervasive, closely-spaced fractures provide increased permeability and fluid/gas throughput. Dickite is nearly always closely associated with strongly silicified zones. In the White Horse cell (G, Plate 2), dickite occurs in a crude ring around the zones of kaolinite and alunite which form the center of the cell.

Calcite and epidote of the distal, pyrite-poor areas of the propylitically altered wall rocks around the Big Rock Candy Mountain cell are well exposed along the Sevier River in Marysvale Canyon (C, Plate 2). One kilometer north of Big Rock Candy Mountain (D, Plate 2), pyrophyllite was mapped along a narrow, ENE-trending fracture zone. The presence of this mineral was confirmed via XRD analysis. Pyrophyllite, a high temperature clay mineral in the kaolinite group, had not been identified in the Antelope range prior to this study. The fracture zone could be a part of a system of radial fractures emanating from the Central Intrusive stocks.

A majority of the alunites in the Antelope Range are K-rich and were formed 23 m.y. ago. However, several of the alunite mines in the district are rich in natroalunite, the Na-rich end member of the K-Na alunite isomorphous series. The Na-rich alunite has been dated at 14 m.y. and is superimposed as veins and lenses upon the K-alunite in certain areas of the Big Star, Yellow Jacket, and Al Kee Mee cells (Cunningham, 1984). Natroalunite was detected with the AVIRIS data in the documented natroalunite mines located at the south end of the Big Star cell (E, Plate 2). Aerial mixtures of K- and Na-rich alunite in the Yellow Jacket mine at the center of the Yellow Jacket cell were mapped as "intermediate composition" alunite (F, Plate 2). Figure 6 shows laboratory reference spectra of alunites from the K-Na isomorphous series. It is evident that the primary Al-OH absorption features shift to longer wavelengths and become narrower with increasing Na content. Similar spectral variations are present in AVIRIS spectra of alunites from the Antelope Range. Figure 7 shows an average AVIRIS spectrum sampled from the Big Star natroalunite mine, and a spectrum of K alunite sampled from the advanced argillic alteration zone of the Yellow Jacket cell. The K alunite spectrum shows evidence of jarosite, as indicated by the feature at 2.27 microns.

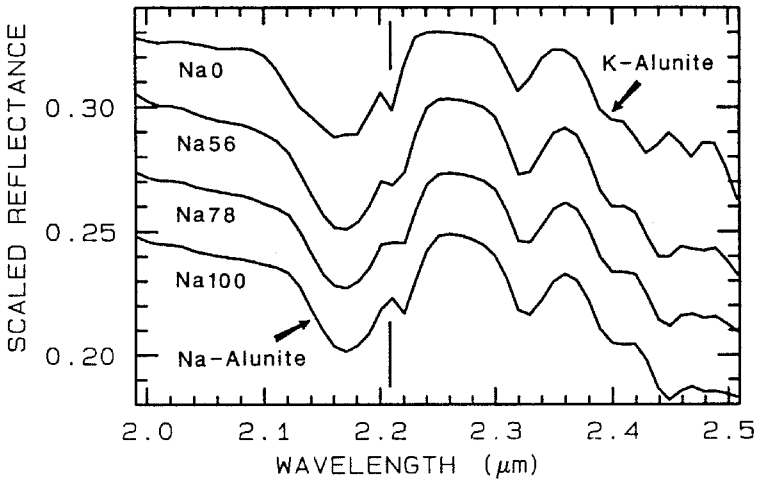

Figure 6. Laboratory spectra of the K-Na alunite isomorphous series. From Swayze (1997).

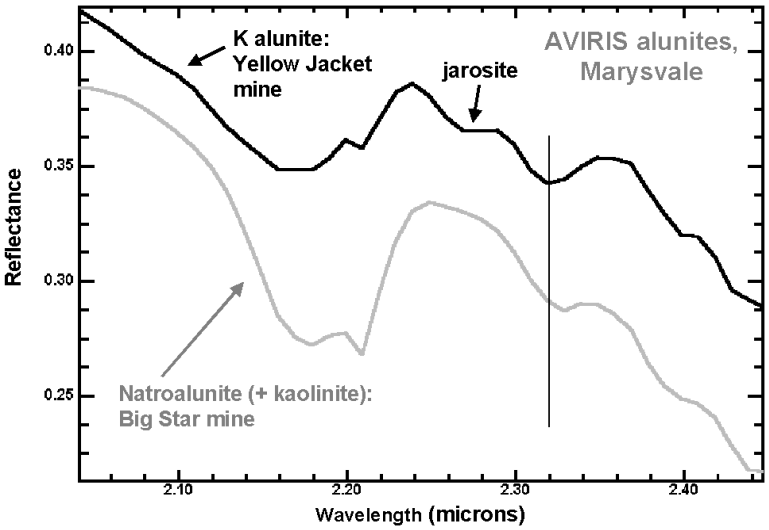

Figure 7. Average AVIRIS spectra of K and Na alunites from the Antelope Range.

The mineral topaz ($Al_2[SiO_4](OH,F)_2$) was detected in parts of the Big Rock Candy Mountain and Yellow Jacket cells with the AVIRIS mapping. Topaz is another mineral not previously documented in this district. Figure 8 shows a laboratory spectrum measured from a rounded cobble found in a dry wash along the southeastern flank of the Yellow Jacket cell. The deep absorption band at 2.088

microns is diagnostic of topaz. XRD analysis has indicated that this rock contains topaz, dickite and kaolinite. The AVIRIS-based mineral mapping detected topaz in scattered pixels in the southern part of the Yellow Jacket cell, some of which are within several hundred meters of the sample collection site. An average AVIRIS spectrum of pixels mapped as topaz with the AVIRIS data is also shown in Figure 8. Topaz is commonly found in veins and vugs in acidic igneous rocks, and is usually produced by pneumatolytic, or gaseous, alteration processes occurring in the later stages of an intrusive event (Deer et al., 1966).

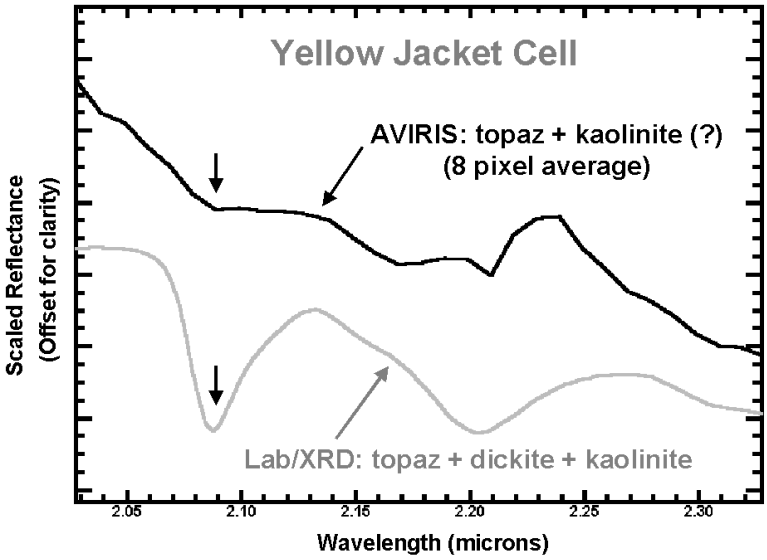

Figure 8. Laboratory and average AVIRIS spectra of intimate mixtures of topaz, kaolinite and dickite from the Yellow Jacket cell.

7. Conclusions

Due to the downcutting of the Sevier River, the epithermal acid sulfate hydrothermal systems of the Marysvale volcanic field are ideally exposed for three dimensional reconstruction of the geothermal and geochemical regimes responsible for their genesis. Several minerals previously un-documented in the Antelope Range were mapped with the AVIRIS data, showcasing the ability of imaging spectroscopy to detect subtle variations in mineralogy which are often difficult and time consuming to recognize using traditional field and laboratory techniques.

The ability of the AVIRIS/Tetracorder combination to differentiate K- versus Na-rich alunites was confirmed. This study also demonstrated the spectral separability of jarosites formed by different processes. Jarosite in exposed propylitic alteration zones formed by supergene oxidation of disseminated pyrite was differentiated from jarosite in advanced argillic alteration zones formed by the oxidation of hypogene H_2S in a steam-heated hydrothermal environment. XRD results showing a lack of pyrite in rocks containing jarosite sampled from the argillic alteration zone of the Yellow Jacket cell appear to support a hypogene origin for the jarosites there, as proposed in a genetic model of the replacement alunite deposits (Cunningham et al., 1984). The spectral separability of supergene and hypogene jarosite has important implications for both mineral exploration and AML applications.

This study for the first time accurately mapped the distribution of jarosite in the Antelope Range. From an environmental standpoint, the presence of these large exposures of non-anthropogenic jarosite make the Antelope Range an ideal site in which to study the effects of natural acid drainage in a district with relatively low concentrations of metals available for transport.

7. References

Clark, R.N., A.J. Gallagher, and G.A. Swayze, 1990, "Material absorption band depth mapping of imaging Spectrometer data using a complete band shape least-squares fit with library reference spectra," in Proceedings of the Second Airborne Visible/Infrared Imaging Spectrometer (AVIRIS) Workshop, JPL Publication 90-54, pp. 176-186.

Clark, R.N., G.A. Swayze, A. Gallagher, N. Gorelick, and F. Kruse, 1991, "Mapping with imaging spectrometer data using the complete band shape least-squares algorithm simultaneously fit to multiple spectral features from multiple materials," in Proceedings of the Third Airborne Visible/Infrared Imaging Spectrometer (AVIRIS) Workshop, JPL Publication 91-28, pp. 2-3.

Clark, R.N. and G.A. Swayze, 1995, "Mapping minerals, amorphous materials, environmental materials, vegetation, water, ice and snow, and other materials: The USGS Tricorder Algorithm," in Summaries of the Fifth

Annual JPL Airborne Earth Science Workshop, January 23- 26, Pasadena, CA, R.O. Green, Ed., JPL Publication 95-1, pp. 39-40.

Clark, R.N., G.A. Swayze, T.V.V. King, K.E. Livo, R.F. Kokaly, J.B. Dalton, J.S. Vance, B.W. Rockwell, and R.R. McDougal, 1999, Surface reflectance calibration of terrestrial imaging spectroscopy data: a tutorial using AVIRIS, USGS Open File Report 99-xx. In press. Available online at: **http://speclab.cr.usgs.gov/PAPERS.calibration.tutorial/calibntA.html**

Cunningham, C.G., J.D. Rasmussen, T.A. Steven, R.O. Rye, P.D. Rowley, S.B. Romberger, and J. Selverstone, 1998, "Hydrothermal uranium deposits containing molybdenum and flourite in the Marysvale volcanic field, west-central Utah," Mineralium Deposita, vol. 33, pp. 477-494.

Cunningham, C.G., R.O. Rye, T.A. Steven, and H.H. Menhert, 1984, "Origins and exploration significance of replacement and vein-type alunite deposits in the Marysvale volcanic field, west central Utah," Econ. Geol., vol. 79, no. 1, pp. 50-71.

Deer, W.A., R.A. Howie, and J. Zussman, 1966, *An Introduction to the Rock Forming Minerals*, Longman Group, London, p. 228.

Gao, B.C. and A.F.H. Goetz, 1990, "Column atmospheric water vapor and vegetation liquid water retrievals from airborne imaging spectrometer data," J. Geophys Res. 95, pp. 3549-3564.

Gao, B.C., K.B. Heidebrecht, and A.F.H. Goetz, 1992, ATmospheric REMoval Program (ATREM) User's Guide, version 1.1, Center for the Study of Earth From Space document, University of Colorado, 24pp.

Kerr, P.F., G.P. Brophy, H.M. Dahl, J. Green, and L.E. Woolard, 1957, "Marysvale, Utah, uranium area," Geol. Soc. America Spec. Paper 64, p. 57.

Podwysocki, M.H., D.B. Segal, and M.J. Abrams, 1983, "Use of multispectral scanner images for assessment of hydrothermal alteration in the Marysvale, Utah, mining area," Econ. Geol., vol. 78, pp. 675-687.

Rowley, P.D., C.G. Cunningham, T.A. Steven, H.H. Menhert, and C.W. Naeser, 1998, "Cenozoic igneous and tectonic setting of the Marysvale volcanic field and its relation to other igneous centers in Utah and Nevada," in *Laccolith Complexes of Southeastern Utah: Time of Emplacement and Tectontic Setting - Workshop Proceedings*, J.D. Friedman and A.C. Huffman, Jr., eds., U.S. Geological Survey Bulletin 2158.

Rye, R.O. and C.N. Alpers, 1997, "The stable isotope geochemistry of jarosite," U.S. Geological Survey Open-File Report 97-88.

Swayze, G.A., 1997, "The hydrothermal and structural history of the Cuprite Mining District, Southwestern Nevada: An integrated geological and geophysical approach," Ph. D. Dissertation, University of Colorado, Boulder, Colorado, p. 399.